

Non-isothermal crystallization behavior of dynamically vulcanized long chain branched polypropylene/ethylene-propylene-diene monomer blends

Zinan Zhang¹ · Fengyuan Yu¹ · Wei Yu¹ · Hongbin Zhang¹

Received: 15 June 2015 / Accepted: 16 September 2015 / Published online: 19 September 2015
© Springer Science+Business Media Dordrecht 2015

Abstract The non-isothermal crystallization behaviors of long chain branched isotactic polypropylene (LCB PP), dynamically vulcanized LCB PP/ethylene-propylene-diene monomer (EPDM) blends at various weight ratios were investigated by DSC, rheology and optical microscopy. LCB PP/EPDM blends were found to show a different crystallization behavior in comparison with linear PP/EPDM blends, showing a minimum in the peak temperature of crystallization with increasing the content of EPDM while the latter showing a maximum. The nucleation and the crystallization kinetics of PP were induced and accelerated by long chain branches and EPDM. The acceleration of crystallization kinetics of LCB PP induced by LCB structures was attributed to the grafted efficient nucleation agent. The influence of EPDM on the crystallization combines the effects of enhancement and retardation, depending on its content in the blends. Based on the thermodynamics theory of crystallization, a modified crystallization model was developed to reveal the crystallization mechanism of LCB PP/EPDM blends.

Keywords Crystallization · Polyolefins · Rheology · Thermoplastics · Elastomers

Introduction

Thermoplastic elastomers (TPEs) based on isotactic polypropylene (iPP) and ethylene-propylene-diene monomer (EPDM) have been widely used in the industries in recent years. iPP and EPDM are considered to be strictly immiscible because of the poor interfacial adhesion between them [1–3]. The lack of compatibility results in poor properties and limits the scope of applications of such blends. It has been reported that the compatibility of iPP and EPDM can be improved by dynamic vulcanization [1, 2, 4]. Some relevant investigations have been carried out involving the mechanical and thermal properties [5–7], microstructures [5, 6, 8, 9] and crystallization behaviors [10] of the dynamically vulcanized iPP/EPDM blends. These blends can be melt-processed like thermoplastics and exhibit elasticity similar to that of normal vulcanized rubbers.

In comparison with unvulcanized blends of iPP/EPDM, the mechanical properties of dynamic vulcanized blends of iPP/EPDM, including hardness, yield stress, Young's modulus, percentage elongation, impact strength, flexural strength and flexural modulus, were found to display higher values [11]. These properties are mainly attributed to the specific microstructures in the blends, which consist of a continuous iPP matrix with small vulcanized EPDM component dispersed throughout the matrix. The crosslinking of the EPDM particles stabilizes the morphology of the blends. The increased interfacial adhesion permits the interaction of the stress concentration zone developed from the elastomer particles under deformation, and promotes shear yielding in the PP matrix. A small amount of PP/EPDM graft copolymers are produced by the coupling of radicals during the vulcanization process [4, 11].

Crystallization behavior of TPEs is essentially related to the mechanical properties of the materials. The existence of

✉ Hongbin Zhang
hbzhang@sjtu.edu.cn

¹ Advanced Rheology Institute, Department of Polymer Science and Engineering, School of Chemistry and Chemical Engineering, Shanghai Jiao Tong University, Shanghai 200240, People's Republic of China

EPDM is believed to have a complex influence on the crystallization behavior. Although the thermal properties of the blends are largely governed by crystalline iPP since EPDM is an amorphous polymer, the EPDM component affects the nucleation and growth of the iPP crystals through the interaction between them [2, 12]. The incorporation of the EPDM into iPP spherulites influences the spherulitic morphology by changing their size and number. Ihm et al. [12] observed a decrease of the spherulitic size as a result of addition of EPDM in both unvulcanized and dynamic vulcanized iPP/EPDM blends. Wenig and Asresahegn [13] and Machado et al. [14] found that due to the decrease in the interfacial free energy and the heterogeneous nucleation at the EPDM surfaces, the nucleation density of PP increased with increasing the content of EPDM in a large range. Some investigations indicated that EPDM acted a nucleant agent in unvulcanized [14] and dynamic vulcanized iPP/EPDM blends [11].

Branched, lightly crosslinked chain structures of iPP induced by Dicumyl peroxide (DCP) may also play a role of nucleating agent in the crystallization process of PP [15]. Previously we reported that the introduction of long branched chains (LCBs) onto the backbone of iPP affected the crystallization behavior of iPP significantly [16, 17]. LCB structures benefit for the nucleation thus accelerating the crystallization process of iPP [16–19]. Carreau et al. also found that the addition of long chain branched polypropylene (LCB PP) to the linear PP caused a significant increase in the crystallization temperature of the blended samples [20]. Similar behaviors have also been reported for other crystalline polymers having long branched chain structures, such as LCB polylactide [21, 22] and LCB polycarbonates [23].

Few studies have explored on the crystallization behavior of dynamically vulcanized long chain branched iPP (LCB PP)/EPDM system. Detailed effects of both LCBs and EPDM on the nucleation and the crystallization kinetics of PP still remain unclear. The acceleration of crystallization kinetics of LCB PP could be induced by the long chain branches (LCBs) structures. In the present work, dynamically vulcanized LCB PP/EPDM blends were prepared and their non-isothermal crystallization behaviors were revealed in comparison with that of the dynamically vulcanized linear iPP/EPDM blends.

The final properties of the semi-crystalline polymers and polymer blends depend on the content of crystalline phase and the morphology formed during processing. The ability to model the crystallization process of polymer is essential not only to produce better quality products but also to streamline the manufacturing process. Several analytical methods have been developed to describe the non-isothermal crystallization kinetic of polymers [24–34]. All of these models are derived from the isothermal crystallization kinetics equation, the Avrami equation. Rao and Rajagopal proposed a general quiescent crystallization model, based on thermodynamic theory of crystallization kinetics [35]. Rao model achieves good

simulation for the non-isothermal crystallization of semi-crystalline polymers; however, it ignored the interfacial energy between the amorphous phase and crystalline phase in their theoretical derivation. For semi-crystalline polymer/amorphous polymer blends, this interfacial energy cannot be ignored. In the present work, taking the heterogeneous nucleation into consideration, a modified Rao model was proposed and the non-isothermal crystallization of the dynamically vulcanized LCB PP/EPDM blends was thereby simulated by this modified model. The combined effects of LCBs and EPDM on the crystallization kinetics of PP, and the possible crystallization mechanism were also discussed.

Experimental section

Materials

The materials used in this work were listed in Table 1. EPDM was kindly provided by Dow Chemical Company, Shanghai, China. 2,5-Dimethyl-2,5(tert-butylperoxy) hexane peroxide and pentaerythritol triacrylate (PETA), a kind of multifunctional monomers, were used to prepare LCB PP. DCP was used to prepare dynamically Vulcanized LCB PP/EPDM Blends as a crosslinking agent. In addition, an antioxidant (trademarked as Inganox 1010) obtained from Ciba Specialty Chemicals Corporation, Switzerland, was used to stabilize the iPP samples during the preparation of LCB PP.

Preparation of LCB PP

LCB PP was prepared by modification of the abovementioned commercial iPP through the reactive extrusion processing in a twin screw extruder, equipped with a screw diameter of 25 mm and a length/diameter ratio (L/D) of 41 (ZE 25A, Berstorff GmbH, Germany). The extrusion temperature was set at 180 °C and the rotational speed of the twin screw extruder was 150 rpm. The prepared details have been discussed in our previous work [16, 36]. The topology structure of LCB PP was star shape with entangled polypropylene branches. The component ratios of samples were listed in Table 2. The weight fraction of LCBs in LCB PP sample was 0, 0.06, 0.33 and 0.37, respectively [16]. PP0 was the linear iPP. PP-1, PP-2 and PP-3 were physically mixed blends of PP and PETA, tested as control samples. Purified LCB PP samples were obtained by dissolving PP0, PP1, PP2 and PP3 in xylene at 140 °C for 10 min, and then precipitating in acetone at room temperature. This procedure was repeated twice to completely remove any unreacted PETA monomer and co-polymerized PETA. Finally, the unpurified and purified LCB PP samples (PP0 to PP3), and the control samples (PP-1 to PP-3) were dried overnight in vented oven at 50 °C before measurements.

Table 1 Materials and characteristics

Materials	Properties	Sources
Isotactic polypropylene (iPP)	MFI=3.0 g/10 min(2.16 kg,230 °C), $M_n=8.0 \times 10^4$, $M_w=3.3 \times 10^5$, Isotacticity \geq 96 %	T300, Shanghai Petrochemical Corporation, China.
Ethylene-propylene-diene rubber (EPDM)	Mooney viscosity/ML1+4(125 °C)=45, Density=0.88 g ml ⁻¹ , Ethylene=70 wt%, ENB=0.5 wt%	Nordel 3745P, Dow Chemical Company, Shanghai, China
2,5-Dimethyl-2,5(tert- butylperoxy) hexane peroxide	Half-life time=1 min at 180 °C	Sinopharm Chemical Reagen, China
pentaerythritol triacrylate (PETA)	/	Sinopharm Chemical Reagen, China
Bis(1-methyl-1-phenylethyl) peroxide (DCP)	Half-life time=1 min at 171 °C	Sigma-Aldrich Corporation, USA

Preparation of dynamically vulcanized LCB PP/EPDM blends

The dynamic vulcanization was carried out in a HAAKE internal mixer (Rheocord 90, HAAKE GmbH, Germany) with a chamber volume of 60 cm³. The mixer temperature was kept at 180 °C. A constant rotor speed of 75 rpm was applied. The purified LCB PP sample prepared in advance was first added and then EPDM was introduced in 1.5 min. After mixing for 2 min, cross-linking agent DCP (1 wt % of EPDM) was added with continuously mixing for 4 min. Four LCB PP samples (PP0, PP1, PP2 and PP3) were used to blend with EPDM at various weight ratios. The formulations of samples were listed in Table 3. The resulting blends were compressed in sheets of 1 mm in thickness on a hot-stage under a pressure of 10 MPa at 190 °C.

Characterizations

DSC measurements

The quiescent crystallization experiments with a constant cooling rate were performed using DSC (PYRIS-1, Perkin Elmer Inc., USA). The samples weighting around 5 mg were heated up rapidly at a rate of 50 °C min⁻¹ to 200 °C, and then held at this temperature for at least 5 min to completely erase any thermal history. After that, the samples were cooled quickly at a

rate of 50 °C min⁻¹ until the temperature reached 180 °C, then cooled from 180 to 80 °C at the rate of 5, 3 and 1 °C min⁻¹. All these processes were executed under nitrogen atmosphere.

Rheological measurements

Rheological experiments were performed using a parallel plates rheometer (Genemi 200HR, Bohlin, UK), in non-isothermal steady shear mode with parallel plates geometry (25 mm in diameter). After holding at 200 °C for 5 min, the non-isothermal steady shear flow at 0.01 s⁻¹ started to operate on the samples and the temperature was controlled to decrease from 200 to 180 °C at a rate of 50 °C min⁻¹, and then cooled from 180 to 80 °C at a rate of 5 °C min⁻¹.

Optical microscope observation

The crystal morphology of non-isothermal crystallization process of the dynamically vulcanized blends was observed by an optical microscope (Leica DMLP, Leica Microsystems GmbH, Germany) with an automatic hot-stage (Linkam TH960, Linkam Scientific Instruments Ltd., UK) equipped with a CCD camera. After holding at 200 °C for 5 min, the samples were cooled quickly at a rate of 50 °C min⁻¹ until the temperature reached 180 °C, then cooled from 180 to 80 °C at the rate of 5 °C min⁻¹.

Table 2 Components of LCB PP samples (parts by weight)

Samples	PP	Irganox 1010	2,5-Dimethyl-2,5(tert- butylperoxy) hexane peroxide	PETA	Weight fractions of LCBs
PP0	100	0.2	0.1	0	0
PP1	100	0.2	0.1	0.5	0.06
PP2	100	0.2	0.1	1	0.33
PP3	100	0.2	0.1	1.5	0.37
PP-1	100	0	0	0.5	–
PP-2	100	0	0	1	–
PP-3	100	0	0	1.5	–

Table 3 Formulation and abbreviation of LCB PP/EPDM samples (parts by weight)

Sample	LCB PP0	LCB PP1	LCB PP2	LCB PP3	EPDM	DCP
PP0 ₉₀ EPDM ₁₀	90				10	0.1
PP0 ₈₀ EPDM ₂₀	80				20	0.2
PP0 ₇₀ EPDM ₃₀	70				30	0.3
PP0 ₆₀ EPDM ₄₀	60				40	0.4
PP0 ₅₀ EPDM ₅₀	50				50	0.5
PP0 ₄₀ EPDM ₆₀	40				60	0.6
PP1 ₈₀ EPDM ₂₀		80			20	0.2
PP1 ₆₀ EPDM ₄₀		60			40	0.4
PP1 ₄₀ EPDM ₆₀		40			60	0.6
PP2 ₈₀ EPDM ₂₀			80		20	0.2
PP2 ₆₀ EPDM ₄₀			60		40	0.4
PP2 ₄₀ EPDM ₆₀			40		60	0.6
PP3 ₉₀ EPDM ₁₀				90	10	0.1
PP3 ₈₀ EPDM ₂₀				80	20	0.2
PP3 ₇₀ EPDM ₃₀				70	30	0.3
PP3 ₆₀ EPDM ₄₀				60	40	0.4
PP3 ₅₀ EPDM ₅₀				50	50	0.5
PP3 ₄₀ EPDM ₆₀				40	60	0.6

Results and discussion

DSC measurements

The DSC cooling curves of the purified and unpurified LCB PP samples (PP0 to PP3), and the control samples (PP-1 to PP-3) were shown in Fig. 1. As shown in Fig. 1a, the peak temperature of crystallization (T_c) of unpurified LCB PP samples increased with the chain branched level. The nuclei density in LCB PP has been observed increasing with the chain branched level [16], which implied that the shift in T_c for LCB PP samples could be attributed to some new nucleation mechanisms. Our previous work showed that although LCBs increased the chain-folding energy of PP chains thereby hindering them from folding back into crystal lamellas, this negative effect on the crystallization rate was offset by the acceleration in nucleation process in the presence of LCBs [37]. With the same addition of PETA, the unpurified LCB PP samples had a similar T_c with the control samples, which indicated a promotion effect of PETA on the nucleation process of iPP. Previously we proved that the PETA were grafted onto PP backbone during the reactive extrusion processing [36]. When monomer (PETA in our experiments) was used, β -scission of iPP was restrained because monomers were grafted onto iPP backbone, which can stabilize iPP macroradicals. Therefore, the effect of the less likely chain β -scission caused by DCP on crystallization behavior of iPP was neglected in present research. To further verify the effect of LCB on crystallization behavior, the purified grafted samples were compared with linear PP samples. The purification process would

remove the unreacted PETA monomers and co-polymerized PETA, only retaining the grafted PETA in the LCB PP samples. As shown in Fig. 1b, the crystallization peaks of the purified LCB PP samples slightly shifted to lower temperatures compared with unpurified samples due to the reduction in the PETA content. Therefore, combining the results shown in Fig. 1a and b, as the chain branched level increases, the crystallization capability of LCB PP is enhanced rather than weakened in the presence of LCB structures, or more explicitly speaking, the existence of the grafted PETA on the backbone of LCB structures is the main reason that enhances the crystallization capability of LCB PP.

The influences of the component of LCB PP along with its degree of long chain branching, and the content of EPDM on the crystallization behaviors of the blends of PP/EPDM were estimated by the variations of their thermal properties from DSC measurements. Figure 2 showed the thermograms of the four dynamically vulcanized PP/EPDM blends (PP0/EPDM, PP1/EPDM, PP2/EPDM and PP3/EPDM) with different weight fractions of long branched chain (0, 0.06, 0.33 and 0.37, corresponding to PP0, PP1, PP2 and PP3, respectively) at three weight ratios of PP to EPDM (40/0, 60/40 and 80/20). It was found that the existence of LCB PP component significantly increased the T_c of the blends, and that at a certain concentration of EPDM, T_c increased with the degree of long chain branching (here, i.e., the weight fraction of LCBs in PP). As shown in Fig. 3, the appearance of LCBs in PP increased T_c sharply, when the weight fractions of LCBs were less than 5 wt %. However, further rise of LCBs content only slightly increased T_c . In addition, the values of T_c of the three LCB PP/

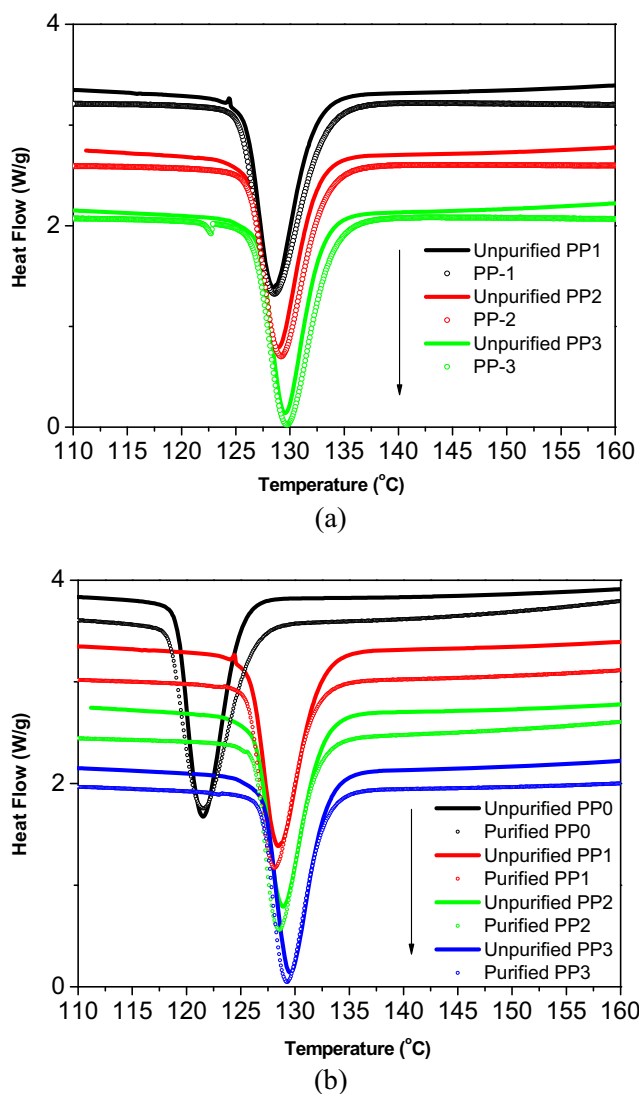


Fig. 1 DSC cooling curves of the purified and unpurified LCB PP samples, and the control samples at the cooling rate of 5 °C min⁻¹

EPDM blends were much higher than that of PP0/EPDM system. Considering that EPDM is an amorphous polymer, the broad crystallization peak is mainly related to the contribution of PP crystallization; this fact strongly implies that the crystallization of the PP in blends is promoted by LCBs and that the nuclei induced by LCB structures can form at a higher temperature, resulting in the increase of *T_c*.

Optical microscope observation

It is obvious that PP3/EPDM blends are able to form crystals much earlier than PP0/EPDM blends. At the same weight ratio, the nuclei density in PP3/EPDM was much higher than that in PP0/EPDM even though the corresponding micrographs were taken at a relatively higher temperature. This result confirmed the nucleation effect of LCBs as observed in DSC experiments (Figs. 2 and 4). For LCB PP/EPDM

blends, it is difficult to observe the spherulite growth process because this process becomes very short. Taking into account that the effect of LCBs on the spherulite growth process is not distinct, the LCBs are considered to promote the overall crystallization process by accelerating the nucleation process and increasing nucleation density.

However, for a certain linear or LCB PP/EPDM blend, the influence of EPDM content on the crystallization behavior of the blend showed a differently special feature. Figure 4c shows the evolution of *T_c* of linear PP0/EPDM and LCB PP3/EPDM blends as a function of EPDM content at some more weight ratios, respectively. The blend of PP3/EPDM displays a completely different crystallization behavior from that of PP0/EPDM system. For PP3/EPDM, the *T_c* first decreases then increases showing a minimum at ca. 30 wt % whereas the *T_c* of PP0/EPDM blend increases with the EPDM content and then decreases showing a maximum at ca. 50 wt %. In fact, results from optical microscopy (Fig. 5) also shed light on these different crystallization behaviors. To investigate the influence of EPDM content on the nucleation process of PP matrix quantitatively, the numbers of nuclei in the view field (*N*) for PP0/EPDM at 130 °C and PP3/EPDM at 135 °C were listed in Table 4. Considering that EPDM is an amorphous polymer, and the changed content of the semi-crystalline polymer PP in the blends, the nuclei density (*D*) in PP matrix in the view field could be roughly calculated as follows:

$$D = \frac{N}{x \cdot A} \tag{1}$$

where *A* is the area of view field and *χ* is the volume fraction of PP component. The calculated values of *D* were listed in Table 4.

For the blends of PP0/EPDM, at the very beginning of crystallization, the values of *N* and *D* increased with the added content of EPDM. However, the overall crystallization rate for the blend at 60:40 (Fig. 5e) is higher than that for the blend at 40:60 (Fig. 5f). For PP3/EPDM blends, it is obvious that the value of *N* decreased with increasing EPDM content, while the value of *D* increased with increasing EPDM content. The overall crystallization rates for the three weight ratios are not so different (Fig. 5g ~ l). These phenomena indicate that the crystallization behavior of PP is influenced by the combined effects of long chain branching and the addition of EPDM.

Rheological measurements

To investigate and furthermore confirm the special non-isothermal crystallization behavior of the dynamically vulcanized blends, rheological experiments were also performed. The evolutions of steady shear viscosities, *η(t)*, with temperature were measured under weak shear flow at a low shear rate

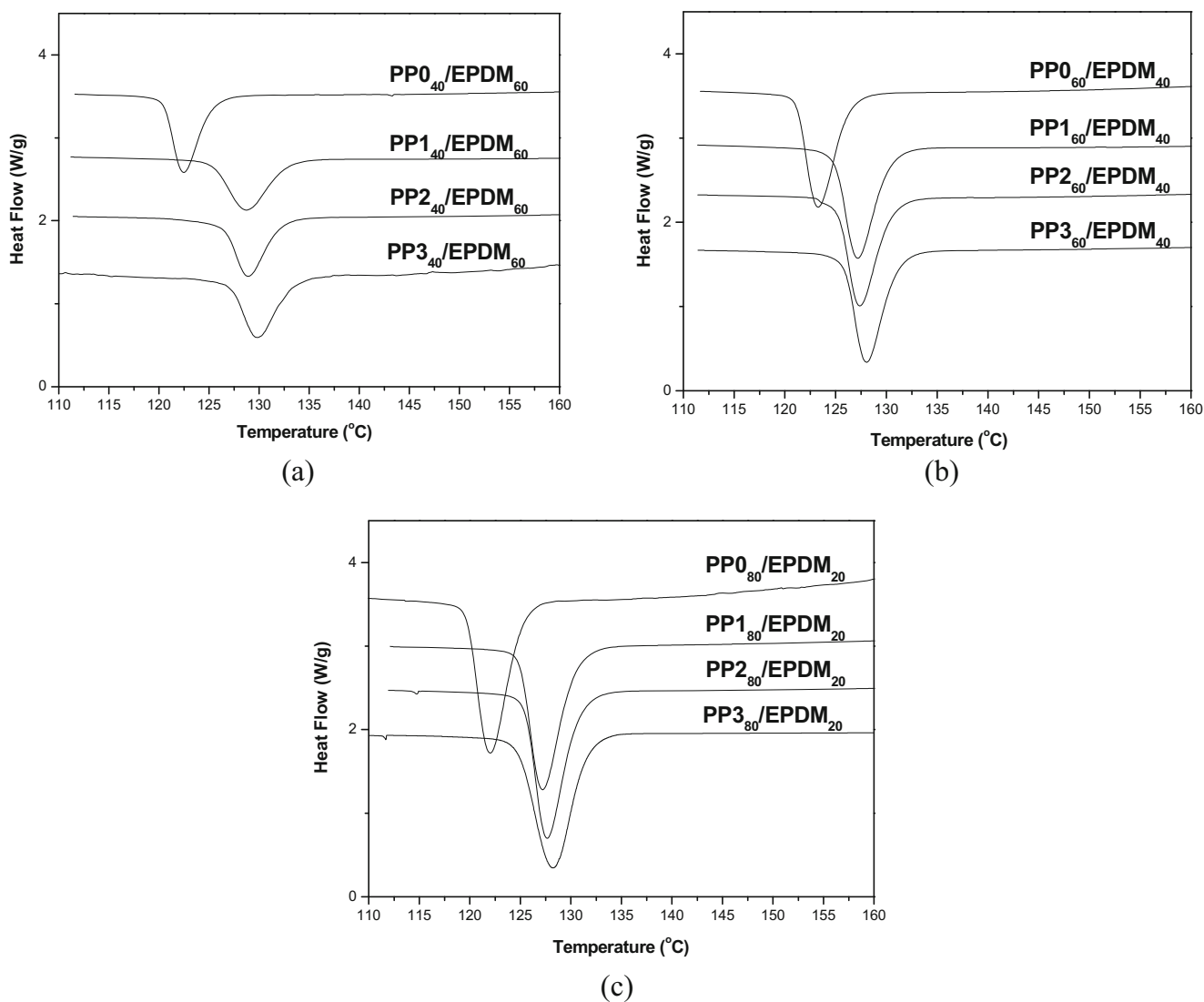


Fig. 2 DSC cooling curves of dynamically vulcanized LCB PP/EPDM blends at various weight ratios: (a) 40:60, (b) 60:40 and (c) 80:20 at a cooling rate of $5\text{ }^{\circ}\text{C min}^{-1}$

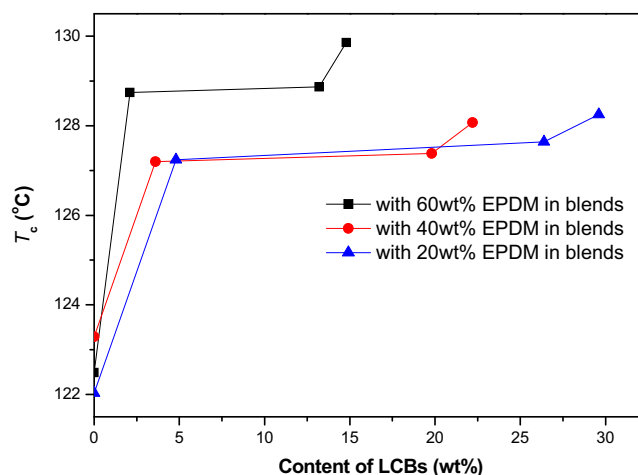


Fig. 3 T_c of PP/EPDM blends as a function of content of LCBs

of 0.01 s^{-1} . The normalized viscosity, η_{norm} , was defined as follow:

$$\eta_{norm} = (\eta(t) - \eta(0)) / (\eta(max) - \eta(0)) \quad (2)$$

where $\eta(max)$ is the max value of $\eta(t)$ and $\eta(0)$ is the minimum value of $\eta(t)$. The normalized viscosities curves for dynamically vulcanized PP0/EPDM and PP3/EDPM blends were shown in Fig. 6a and b, in which the sharp increase of the value of η_{norm} was mainly caused by the occurrence of crystallization of PP on cooling. The values of peak temperature of crystallization measured by rheological experiments (T_{cr}) were calculated from second derivative of the normalized viscosities curves.

The evolution of T_{cr} for either PP0/EPDM or PP3/EDPM blends is in good agreement with that from DSC as shown in Fig. 4c for comparison, though T_{cr} is smaller in value at the

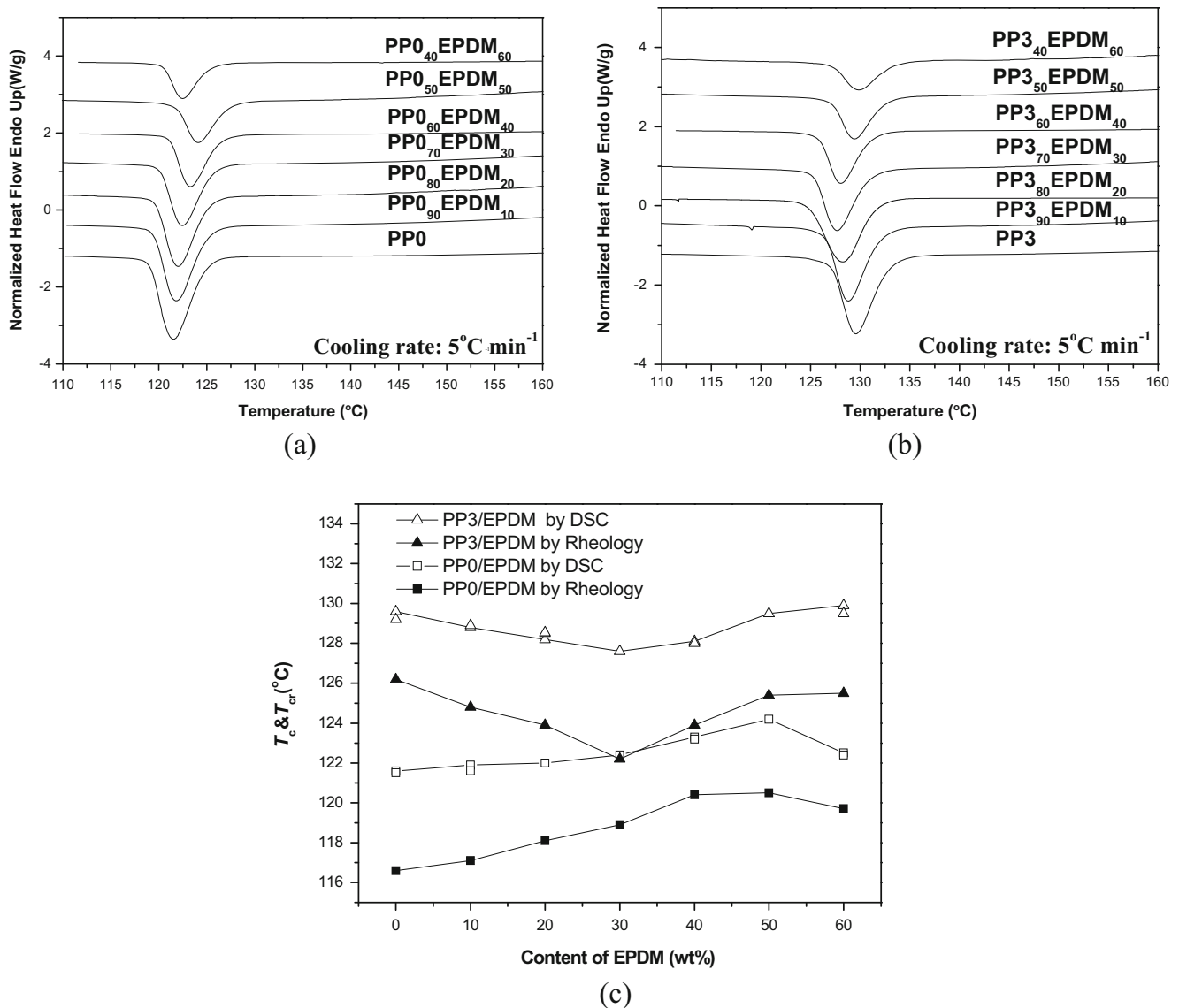


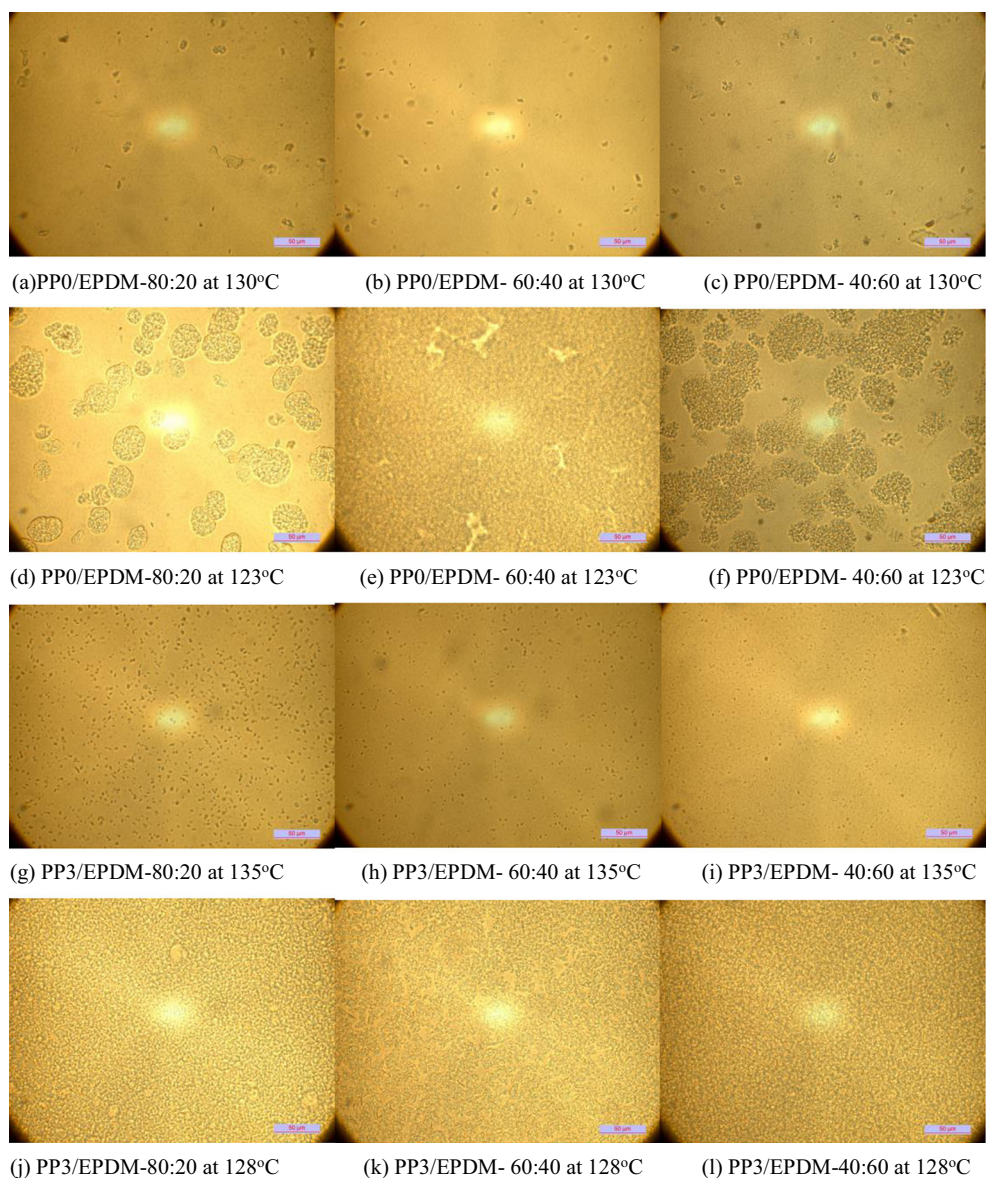
Fig. 4 Cooling curves of PP0/EPDM (a) and PP3/EPDM (b) blends at various weight ratios and (c) peak temperature of crystallization of PP0/EPDM and PP3/EPDM blends measured by DSC and rheology, respectively, as a function of content of EPDM

same weight ratio. Here the differences in the crystallization temperatures between rheological and DSC measurements should be attributed to the different sensitivities and detection mechanisms of rheological and DSC tests. DSC can detect the exothermic signals at the very beginning of crystallization, but the rheometer can only respond when the crystals grow bigger and more enough to result in a detectable increase in viscosity.

During the dynamic vulcanization process, the existence of PP-co-EPDM graft copolymer has been proved [4, 11]. The addition of EPDM in PP will accelerate the nucleation process and increase nucleation density due to the decrease in the surface free energy and due to the heterogeneous nucleation at the EPDM surfaces [13, 14]. However, the EPDM component can also inhibit the growth of spherulites and decrease the spherulite size of PP, due to the incorporation of EPDM into

PP spherulites and the existence of PP-co-EPDM graft copolymers produced in the system [4, 11, 12, 38, 39]. For PP0/EPDM blends, the nuclei densities were low (as shown in Fig. 5 and Table 4), and the values of D increased from 645 to 2945 as the EPDM content increasing from 20 to 60 wt %, indicating that the occurrence of nuclei were mainly induced by the EPDM surfaces. However, excess EPDM retarded spherulite growth of PP. This hindrance effect became more significant when the content of EPDM was larger than 50 wt %. Especially at 60 wt %, the net effect of EPDM on the crystallization of PP is that the negative effect of EPDM on spherulite growth predominates over the positive effect on the promotion of nucleation, thus resulting in the decrease of T_c . Consequently, a maximum was observed in both T_c and T_{cr} curves (Fig. 4c).

Fig. 5 Optical microscope micrographs of dynamically vulcanized PP0/EPDM blends at weight ratios of (a, d) 80:20, (b, e) 60:40 and (c, f) 40:60 at 130 °C and 123 °C, and dynamically vulcanized PP3/EPDM blends at weight ratios of (g, j) 80:20, (h, k) 60:40 and (i, l) 40:60 at 135 °C and 128 °C (Cooling rate: 5 °C min⁻¹)



For LCB PP/EPDM blends, the nucleation induced by LCB structures played a dominant role when the content of LCB PP was high enough (as shown in Fig. 5 and Table 5). The nucleation effect of LCB was prominent in PP blends so that the promotion effect of EPDM on the nucleation of LCB

Table 4 The values of N and D for PP0/EPDM samples at 130 °C and PP3/EPDM samples at 135 °C

Weight ratios	N		D (number mm ⁻²)	
	PP0/EPDM	PP3/EPDM	PP0/EPDM	PP3/EPDM
80/20	48	1068	645	14,416
60/40	81	805	1462	14,566
40/60	108	655	2945	17,867

PP can be ignored at low EPDM concentrations. The main effect of EPDM at such a condition was the inhibition of the spherulites growth of PP through the interactions between EPDM and PP molecules. Furthermore, when the weight fractions of LCBs continually decreased as components of EPDM increased in the blends (as shown in Table 5), the negative retardation of EPDM for PP crystallization became obvious gradually. As a result, the overall crystallization capacity for PP3/EPDM blends decreased as more and more EPDM were added, which can be reflected from the motion trail of crystallization peak on the DSC curves of PP3/EPDM blends. The crystallization peak tended to locate at a lower temperature as the EPDM content was increased as seen in Fig. 4b. However, the decline of crystallization capability was not unlimited. When the weight fraction of EPDM went beyond a certain amount (ca. 30 wt % in the present work), the inducing

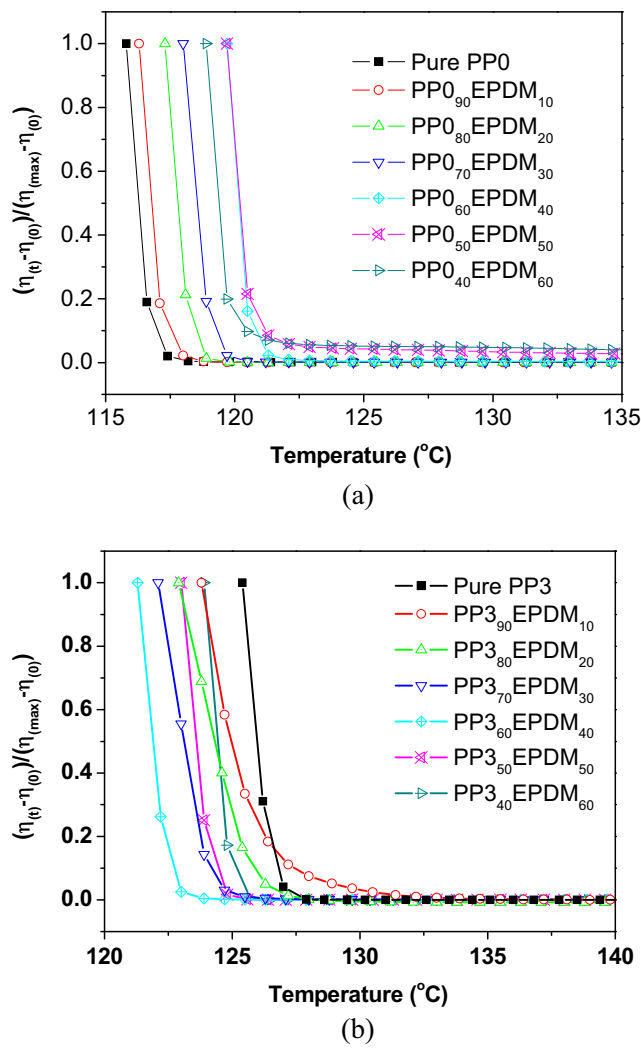


Fig. 6 Normalized viscosity of (a) dynamically vulcanized PP0/EPDM and (b) PP3/EPDM blends at various weight ratios as a function of temperature

nucleation effect of EPDM cannot be ignored. The value of *D* increased up to 17,867 as the EPDM content reached 60 wt %, rising by ca. 20 % compared with that at 20 wt

% or 40 wt % EPDM content. At this high content of EPDM, the rapid increase in the nuclei density indicated that the nucleation can form at a higher temperature, namely, *T_c* shifting to a higher temperature. As a result, it is not surprised to see a minimum in shown in Fig. 4c. Here it must be noted that this increase should also be of limitation because the hindrance effect of EPDM always exists in the system as already clearly revealed for PP0/EPDM blends at high content of EPDM. Therefore, for the LCB PP/EPDM blends in which both components of LCB and EPDM exist, the existence of LCB accelerates the nucleation process of PP, however the EPDM component can accelerates the nucleation process through interface induction and inhibit the spherulite growth of PP at the same time by molecular interaction. This should be the reason that results in different features of the crystallization behaviors of the two kinds of blends of linear PP/EPDM and LCB PP/EPDM. The acceleration of LCB PP to the nucleation process seems to be more effective than that of EPDM, which might be related to lower activation energy of nucleation for the nucleation induced by LCB PP.

Non-isothermal crystallization kinetics

To describe the non-isothermal crystallization kinetic of polymers, some analytical methods have been developed based on Avrami equation [24–26]. Rao and Rajagopal proposed a general quiescent crystallization model based on thermodynamic theory of crystallization kinetics to study non-isothermal crystallization behavior of polymer melts [35]. According to Kim [40] and Choe [41], the crystallization rate $\dot{\alpha}$ can be calculated by using a linear combination of homogeneous and heterogeneous nucleation terms:

$$\dot{\alpha} = \dot{\alpha}_1 + \dot{\alpha}_2 \tag{3}$$

where $\dot{\alpha}_1$ and $\dot{\alpha}_2$ represent the rate of crystallization induced by homogeneous and heterogeneous nucleation, respectively. For blends system, the heterogeneous nucleation term was

Table 5 *T_c* and weight fractions of LCBs for PP0/EPDM and PP3/EPDM blends at various weight ratios at the cooling rate of 5 °C min⁻¹

Weight ratios	PP0/EPDM		PP3/EPDM	
	<i>T_c</i> (°C)	Weight fractions of LCBs (wt%)	<i>T_c</i> (°C)	Weight fractions of LCBs (wt%)
100/0	121.6	0	129.6	37.0
90/10	121.9	0	128.8	33.3
80/20	122.0	0	128.2	29.6
70/30	122.4	0	127.6	25.9
60/40	123.3	0	128.1	22.2
50/50	124.2	0	129.5	18.5
40/60	122.5	0	129.9	14.8

Table 6 Parameters in modified Rao Model for dynamically vulcanized LCB PP/EPDM blends with different cooling rates

Parameters		<i>I</i>	<i>m</i>	<i>N</i>	<i>k</i>	<i>l</i>	<i>k</i> ₁	<i>k</i> ₂	<i>k</i> ₃	<i>μ</i>
<i>β</i>										
PP1/EPDM-80/20	1 °C min ⁻¹	88.6084	1.9792	3.8738	0.8435	0.8775	0.0010	0.6920	2	406.4
	3 °C min ⁻¹	67.6545	1.9244	3.5495	0.6755	0.7524	0.0086	0.3781	2	401.8
	5 °C min ⁻¹	70.1138	1.9800	3.5155	0.6192	0.7523	0.0168	0.2743	2	399.5
PP1/EPDM-60/40	1 °C min ⁻¹	81.1957	1.9396	3.7956	0.9703	0.8687	0.0012	0.4535	2	407.0
	3 °C min ⁻¹	74.1059	1.9541	3.6422	0.6465	0.7919	0.0090	0.3415	2	402.5
	5 °C min ⁻¹	68.8204	1.9623	3.5089	0.6287	0.7702	0.0165	0.2743	2	400.2
PP1/EPDM-40/60	1 °C min ⁻¹	72.0561	1.8504	3.7421	1.0443	0.9182	0.0007	0.2478	2	405.4
	3 °C min ⁻¹	64.7707	1.8776	3.5454	0.6857	0.8134	0.0046	0.2378	2	403.8
	5 °C min ⁻¹	64.2126	1.8826	3.5103	0.6671	0.7943	0.0109	0.2081	2	402.0
PP2/EPDM-80/20	1 °C min ⁻¹	55.8345	1.7672	3.4876	0.9525	0.9257	0.0017	0.8889	2	406.6
	3 °C min ⁻¹	78.7129	1.9850	3.6898	0.6397	0.7591	0.0097	0.3359	2	402.3
	5 °C min ⁻¹	73.5378	1.9983	3.5649	0.5855	0.7688	0.0174	0.3415	2	400.1
PP2/EPDM-60/40	1 °C min ⁻¹	62.7212	1.7983	3.6146	1.0371	0.8436	0.0013	1.1834	2	407.1
	3 °C min ⁻¹	70.9407	1.9351	3.6038	0.6615	0.7796	0.0091	0.3359	2	403.0
	5 °C min ⁻¹	72.9884	2.0105	3.5197	0.6816	0.7226	0.0169	0.3005	2	400.6
PP2/EPDM-40/60	1 °C min ⁻¹	60.8939	1.8000	3.5694	0.9703	0.8793	0.0008	0.4058	2	406.4
	3 °C min ⁻¹	49.6210	1.7624	3.3296	0.6125	0.8435	0.0061	0.4132	2	404.1
	5 °C min ⁻¹	55.4630	1.8525	3.3493	0.6275	0.7722	0.0127	0.2914	2	402.0
PP3/EPDM-80/20	1 °C min ⁻¹	100.655	2.0224	3.9984	0.8737	0.8733	0.0019	0.4535	2	407.7
	3 °C min ⁻¹	62.2464	1.8850	3.4769	0.7699	0.6718	0.0099	0.2551	2	403.0
	5 °C min ⁻¹	77.9603	2.0221	3.6461	0.5800	0.7770	0.0185	0.2386	2	400.5
PP3/EPDM-60/40	1 °C min ⁻¹	74.8436	1.8982	3.7361	0.9643	0.8698	0.0014	0.4535	2	407.5
	3 °C min ⁻¹	51.4631	1.8039	3.3081	0.7805	0.7341	0.0106	0.3781	2	403.4
	5 °C min ⁻¹	67.2489	1.9725	3.4539	0.6407	0.7820	0.0168	0.2743	2	401.1
PP3/EPDM-40/60	1 °C min ⁻¹	66.8666	1.8187	3.6804	0.9536	0.9677	0.0008	1.6529	2	408.5
	3 °C min ⁻¹	57.4870	1.8304	3.4377	0.7153	0.7618	0.0065	0.3415	2	404.5
	5 °C min ⁻¹	58.2183	1.8646	3.4094	0.6104	0.7460	0.0138	0.2743	2	402.4

ignored by Rao model, and $\dot{\alpha}_1$ can be calculated by Rao model. Based on the first and the second law of thermodynamics, the simplified Rao model can be expressed as follows:

$$\dot{\alpha}_1 = I \left(\frac{2T(T_m^0 - T)}{T_m^0(T_m^0 + T)} \right)^m \left(\frac{T - T_g}{T_m^0} \right)^n \left(\frac{\alpha}{\alpha_0} \right)^k \left(1 - \frac{\alpha}{\alpha_0} \right)^l \quad (4)$$

where *I*, *m*, *n*, *k*, and *l* are constants, *T*_m⁰ and *T*_g refer to the equilibrium melting temperature and the glass transition temperature of materials, respective, and α represents the degree of crystallinity at temperature *T* while α_0 stands for the ultimate absolute crystallinity.

Assumption that

$$\dot{\alpha}_2 = k_1 \exp \left[-k_2 (T - \mu)^{k_3} \right] \quad (5)$$

where *k*₁, *k*₂, *k*₃ and μ are constants, *k*₁ is the crystallization kinetics constant for $\dot{\alpha}_2$ and μ is related to the inducing

temperature of heterogeneous nucleation. According to Eqs. (4) and (5), the crystallization rate of polymer blends $\dot{\alpha}$ can be obtained by the following equation:

$$\dot{\alpha} = I \left(\frac{2T(T_m^0 - T)}{T_m^0(T_m^0 + T)} \right)^m \left(\frac{T - T_g}{T_m^0} \right)^n \left(\frac{\alpha}{\alpha_0} \right)^k \left(1 - \frac{\alpha}{\alpha_0} \right)^l + k_1 e^{1 \cdot Xp} \left[-k_2 (T - \mu)^{k_3} \right] \quad (6)$$

This modified Rao equation was used to model the non-isothermal crystallization of polymer blends.

For the convenience of solving Eq. (6), the second term is ignored temporarily. The relative degree of crystallinity, *X*, is the ratio of α and α_0 . And then the $\dot{\alpha}$ can be expressed as follows:

$$X = \frac{\alpha}{\alpha_0} \rightarrow \dot{\alpha} = \frac{dX}{dt} \quad (7)$$

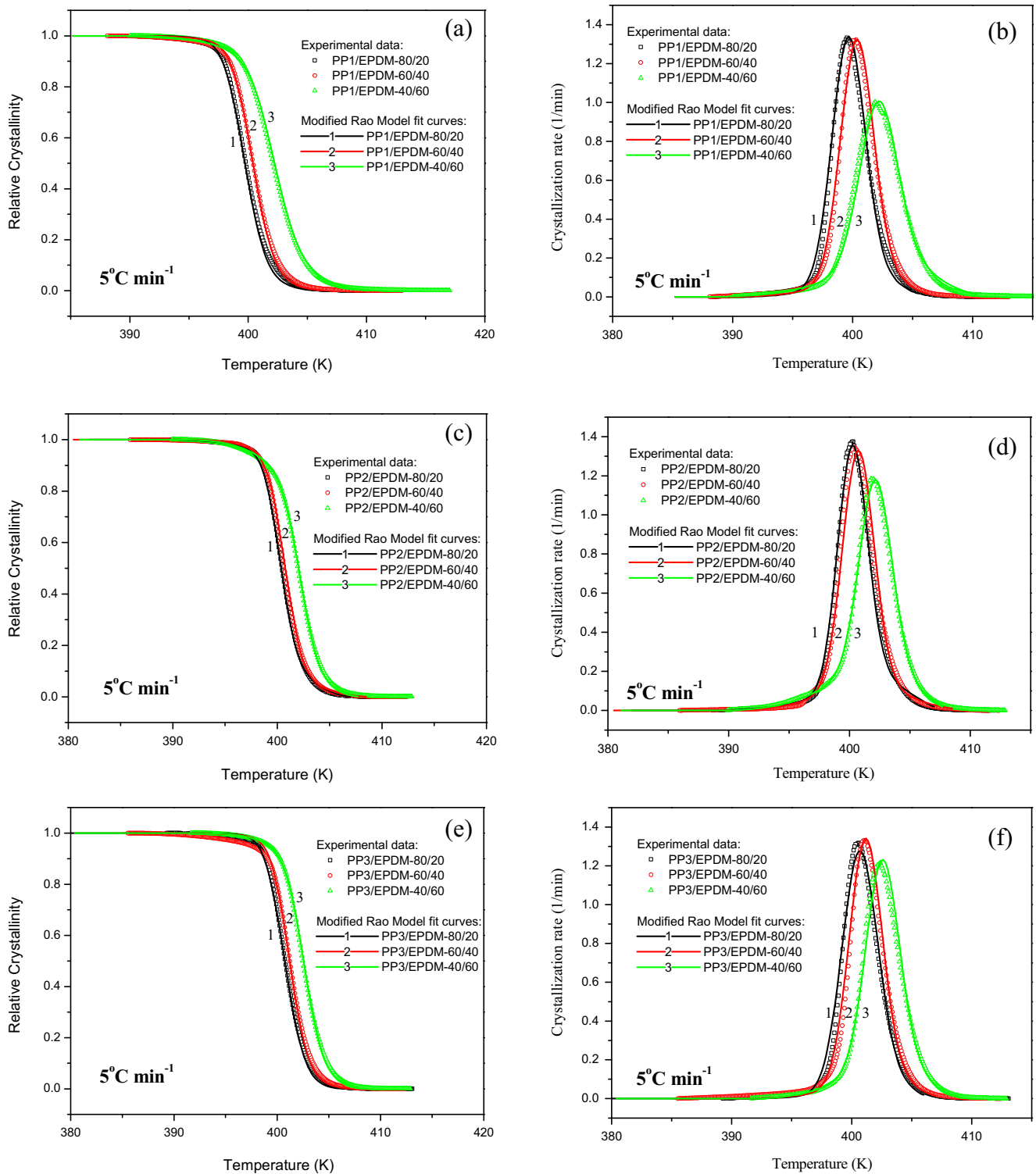


Fig. 7 Plots of relative crystallinity versus temperature and crystallization rate versus temperature for dynamically vulcanized LCB PP/EPDM blends at different weight ratios and a cooling rate of 5 °C min⁻¹ predicted by modified Rao Model

This quiescent crystallization equation can be modified in order to describe non-isothermal crystallization

[29, 30, 42]. For non-isothermal crystallization at a chosen cooling rate, the relative crystallinity, X , is a

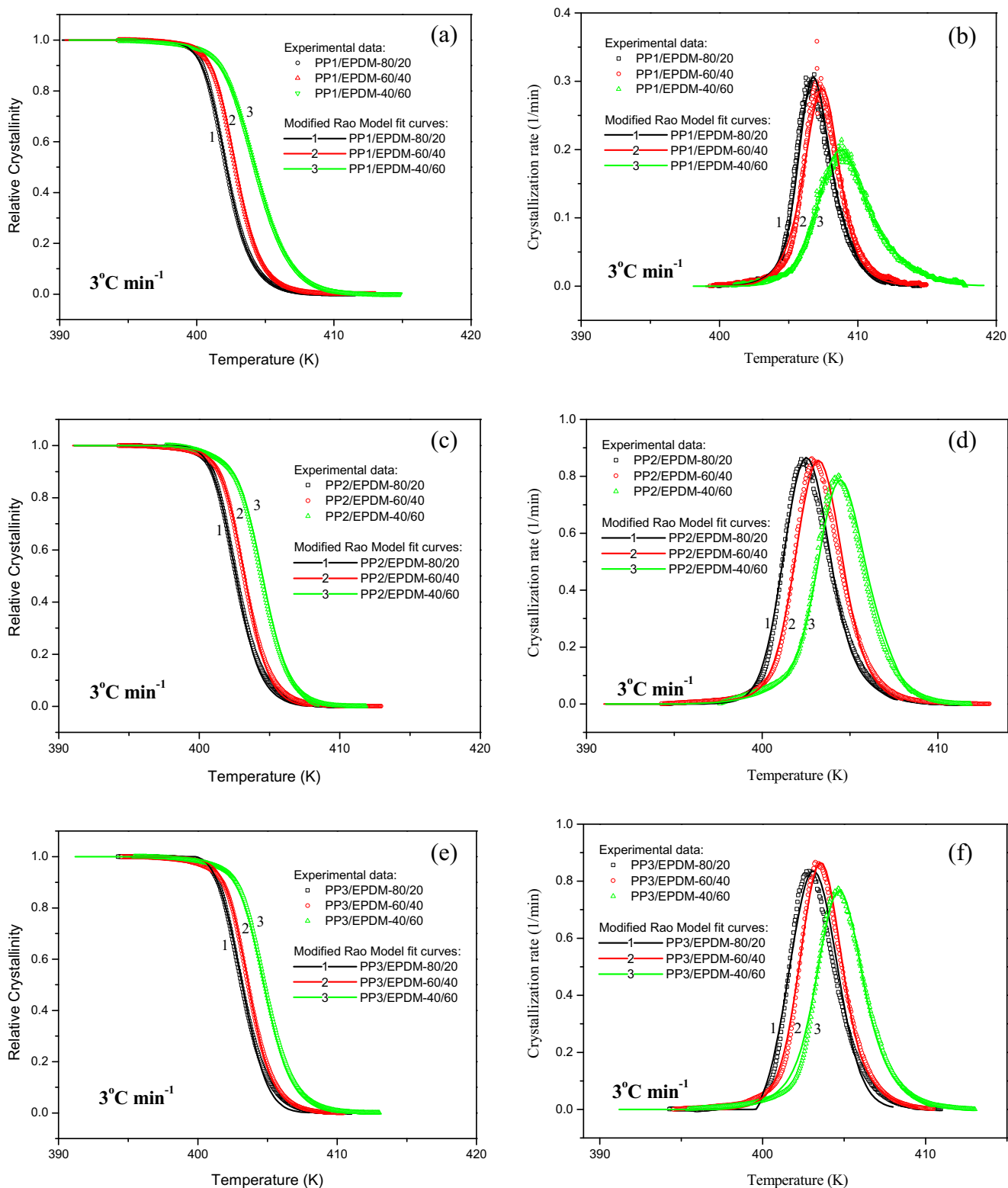


Fig. 8 Plots of relative crystallinity versus temperature and crystallization rate versus temperature for dynamically vulcanized LCB PP/EPDM blends at different weight ratios and a cooling rate of 3 °C min⁻¹ predicted by modified Rao Model

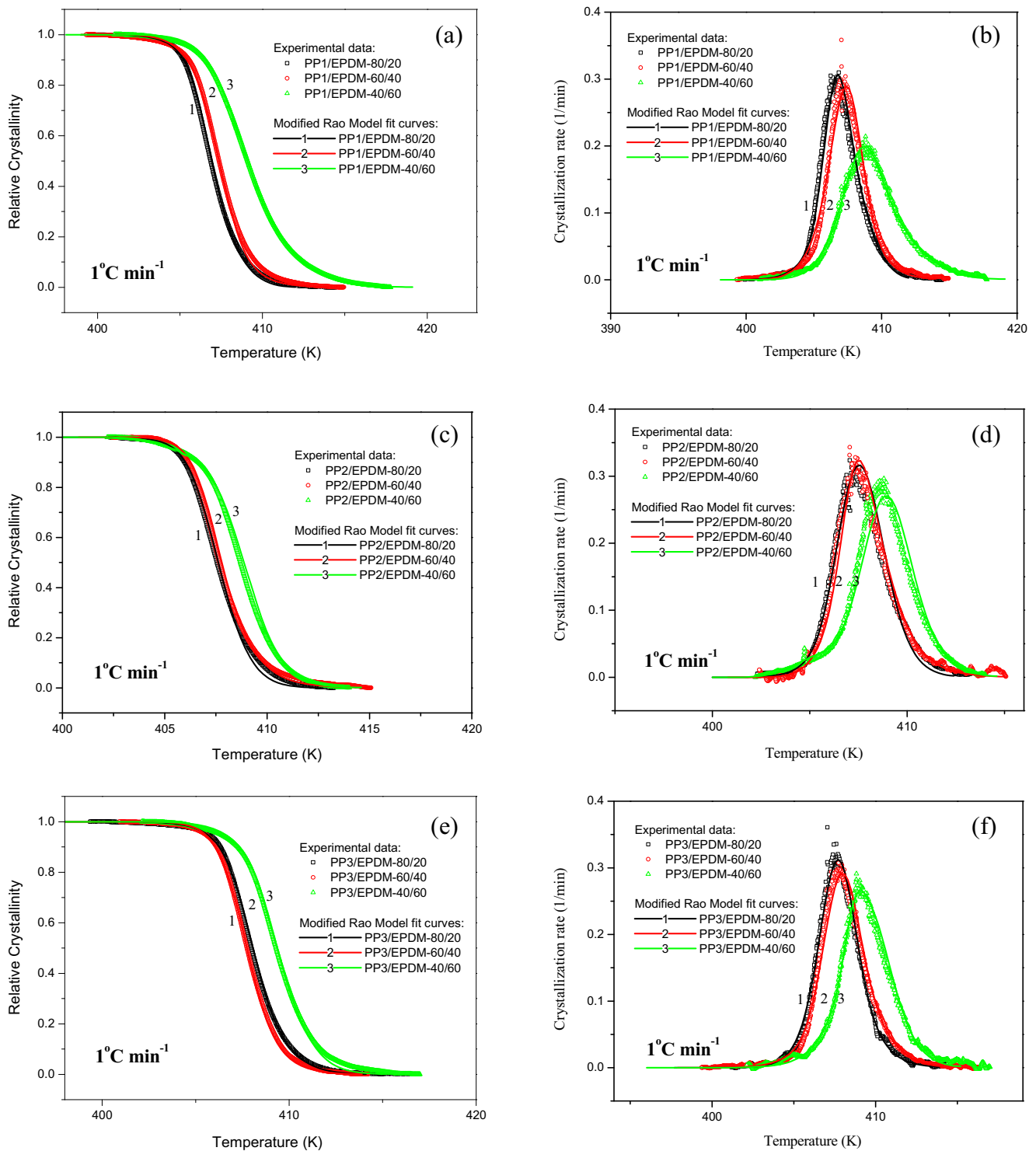


Fig. 9 Plots of relative crystallinity versus temperature and crystallization rate versus temperature for dynamically vulcanized LCB PP/EPDM blends at different weight ratios and a cooling rate of 1 °C min⁻¹ predicted by modified Rao Model

function of crystallization temperature, and Eq. (7) can be rewritten as

$$X = \frac{\int_{T_0}^T (dH_c/dT)dT}{\int_{T_0}^{T_\infty} (dH_c/dT)dT} \quad 0 < X_c \leq 1 \quad (8)$$

where T is the crystallization temperature, T_0 and T_∞ represent the onset and end crystallization temperatures, respectively.

Assumption that:

$$\beta = \pm \frac{dT}{dt} \quad (9)$$

where β refers to the rate of temperature changing (heating to take positive and cooling to take negative). By substituting Eqs. (7) ~ (9) into Eq. (4), the following expression of Rao model can be obtain:

$$\pm\beta \frac{dX}{dT} = I \left(\frac{2T(T_m^0 - T)}{T_m^0(T_m^0 + T)} \right)^m \left(\frac{T - T_g}{T_m^0} \right)^n X^k (1-X)^l \quad (10)$$

Equation (10) in logarithm is as follows:

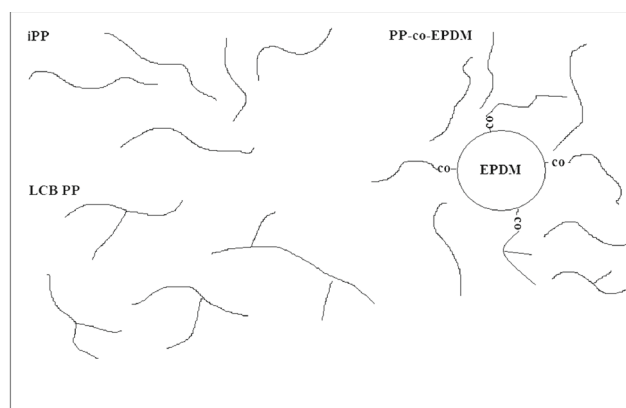
$$\ln \left(\pm\beta \frac{dX}{dT} \right) = \ln I + m \ln \left(\frac{2T(T_m^0 - T)}{T_m^0(T_m^0 + T)} \right) + n \ln \left(\frac{T - T_g}{T_m^0} \right) + k \ln X + l \ln(1-X) \quad (11)$$

The values of constant parameters I , m , n , k , and l can be calculated by using least square method according to Eq. (11). By substituting these values into Eq. (6), the values of k_1 , k_2 , k_3 and μ can be obtained. The detailed values of these parameters were listed in Table 6. The simulation results of modified Rao model were shown in Figs. 7, 8 and 9.

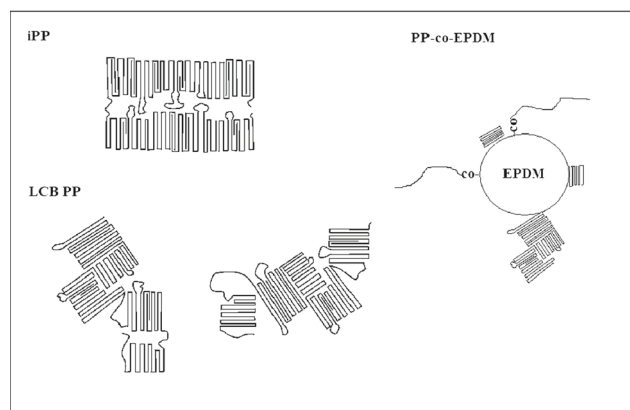
From the Figs. 7, 8 and 9, obviously, for all of the blends at various weight ratios and cooling rates, the predictions in terms of our modified Rao model are in good agreement with the experimental data. It is also found that, for the same blending system at the same weight ratio, the values of μ decrease with the increase of cooling rate. For the different blending systems at the same weight ratio, the values of μ increase with the increase in the content of LCBs, suggesting that the addition of LCBs shorten the induction time of PP crystallization. For the same blending system at the same weight ratio, the values of k_1 increase with the increase in the cooling rate. For the different blending systems with the same weight ratio, the values of k_1 increase with content of LCBs, indicating that the addition of LCBs improves the crystallization kinetics of PP, acting as heterogeneous nucleating agents.

Conclusions

The present work clearly indicates that there are three kinds of crystallization patterns in the LCB PP/EPDM blends: the homogeneous nucleation and crystallization of linear PP, the crystallization induced by LCBs in the PP matrix, and the crystallization induced by EPDM component on the phase interface. The above proposed mechanism is schematically described in Scheme 1. For linear PP, the molecular chains are much easier to orientate and grow into spherulites with big sizes. In contrast, the spherulites induced by LCBs are much smaller having a faster nucleation rate that results in a large nucleation density due to the promotion effect of the



(a)



(b)

Scheme 1 Crystallization patterns for dynamically vulcanized LCB PP/EPDM blends: (a) melting state of dynamically vulcanized LCB PP/EPDM blends and (b) crystallized state of dynamically vulcanized LCB PP/EPDM blends

formation of stable crystallization precursor structures. EPDM component promotes nucleation process but also limits the activities of PP molecules due to the copolymeric structures of PP-co-EPDM. The relationship among the three crystallization patterns is competitive and the dominant pattern depends on the relative content of LCBs and EPDM in the blends. For the PP0/EPDM blends, there are only two crystallization patterns because of the lack of LCBs of PP, which is the essential reason that causes the different crystallization behaviors between linear PP/EPDM and LCB PP/EPDM blends.

Both LCBs of PP and EPDM can induce the nucleation and improve the crystallization kinetics of PP. The addition of EPDM slows down the growth of PP crystals due to the incorporation of EPDM into PP spherulites and the existence of PP-co-EPDM graft copolymers produced in the blends. The combined effects of LCBs of PP and EPDM component make the linear PP/EPDM and LCB PP/EPDM blends exhibit different crystallization behaviors.

Acknowledgments The authors are thankful for the financial support for this work from the National Natural Science Foundation of China (51103084), National Basic Research Program of China (2011CB606005, 2012CB025901) and the Shanghai Leading Academic Discipline Project (No. B202).

References

- Phan TTM, Denicola AJ, Schadler LS (1998) Effect of addition of polyoxypropylenediamine on the morphology and mechanical properties of maleated polypropylene/maleated rubber blends. *J Appl Polym Sci* 68:1451–1472
- Kim BC, Hwang SS, Lim KY, Yoon KY (2000) Toughening of PP/EPDM blend by compatibilization. *J Appl Polym Sci* 78:1267–1274
- Choudhary V, Varma HS, Varma IK (1991) Polyolefin blends effect of EPDM rubber on crystallization, morphology and mechanical properties of polypropylene EPDM blends. *Polymer* 32:2534–2540
- Shen YX, Xie BH, Yang W, Li ZM, Yang MB (2007) Effect of EPDM content on melt flow, microstructures and fracture behavior of dynamically vulcanized PP/EPDM blends. *J Macromol Sci B Phys* 46:1127–1138
- Tang X-G, Yang W, Shan G-F, Yang B, Xie B-H, Yang M-B, Hou M (2009) Effect of temperature gradient on the development of beta phase polypropylene in dynamically vulcanized PP/EPDM blends. *Colloid Polym Sci* 287:1237–1242
- Babu RR, Singha NK, Naskar K (2010) Interrelationships of morphology, thermal and mechanical properties in uncrosslinked and dynamically crosslinked PP/EOC and PP/EPDM blends. *Express Polym Lett* 4:197–209
- Yeh JT, Lin SC (2009) Optimized processing conditions for the preparation of dynamically vulcanized EPDM/PP thermoplastic elastomers containing PP resins of various melt indexes. *J Appl Polym Sci* 114:2806–2815
- Litvinov VM (2006) EPDM/PP thermoplastic vulcanizates as studied by proton NMR relaxation: phase composition, molecular mobility, network structure in the rubbery phase, and network heterogeneity. *Macromolecules* 39:8727–8741
- Wu HG, Ning NY, Zhang LQ, Tian HC, Wu YP, Tian M (2013) Effect of additives on the morphology evolution of EPDM/PP TPVs during dynamic vulcanization in a twin-screw extruder. *J Polym Res* 20:266
- Brostow W, Datashvili T, Hackenberg KP (2010) Effect of different types of peroxides on properties of vulcanized EPDM plus PP blends. *Polym Compos* 31:1678–1691
- Jain AK, Nagpal AK, Singhal R, Gupta NK (2000) Effect of dynamic crosslinking on impact strength and other mechanical properties of polypropylene/ethylene-propylene-diene rubber blends. *J Appl Polym Sci* 78:2089–2103
- Ihm DJ, Ha CS, Kim SC (1988) Crystalline structure and morphology of dynamically cured EPDM and PP blends. *Polymer (Korea)* 12:249–255
- Wenig W, Asresahegn M (1993) The influence of rubber-matrix interfaces on the crystallization kinetics of isotactic polypropylene blended with ethylene-propylene-diene terpolymer (EPDM). *Polym Eng Sci* 33:877–888
- Manchado MAL, Biagiotti J, Torre L, Kenny JM (2000) Polypropylene crystallization in an ethylene-propylene-diene rubber matrix. *J Therm Anal Calorim* 61:437–450
- Wang X, Tzoganakis C, Rempel GL (1996) Chemical modification of polypropylene with peroxide/pentaerythritol triacrylate by reactive extrusion. *J Appl Polym Sci* 61:1395–1404
- Yu FY, Zhang HB, Liao RG, Zheng H, Yu W, Zhou CX (2009) Flow induced crystallization of long chain branched polypropylenes under weak shear flow. *Eur Polym J* 45:2110–2118
- Tian JH, Yu W, Zhou CX (2007) Crystallization behaviors of linear and long chain branched polypropylene. *J Appl Polym Sci* 104:3592–3600
- Agarwal PK, Somani RH, Weng WQ, Mehta A, Yang L, Ran SF, Liu LZ, Hsiao BS (2003) Shear-induced crystallization in novel long chain branched polypropylenes by in situ rheo-SAXS and -WAXD. *Macromolecules* 36:5226–5235
- Wang XD, Zhang YX, Liu BG, Du ZJ, Li HQ (2008) Crystallization behavior and crystal morphology of linear/long chain branching polypropylene blends. *Polym J* 40:450–454
- Tabatabaei SH, Carreau PJ, Ajji A (2009) Rheological and thermal properties of blends of a long-chain branched polypropylene and different linear polypropylenes. *Chem Eng Sci* 64:4719–4731
- Nofar M, Zhu WL, Park CB, Randall J (2011) Crystallization kinetics of linear and long-chain-branched polylactide. *Ind Eng Chem Res* 50:13789–13798
- You J, Lou L, Yu W, Zhou C (2013) The preparation and crystallization of long chain branching polylactide made by melt radicals reaction. *J Appl Polym Sci* 129:1959–1970
- Zhai WT, Yu J, Ma WM, He JS (2007) Influence of long-chain branching on the crystallization and melting behavior of polycarbonates in supercritical CO₂. *Macromolecules* 40:73–80
- Nakamura K, Katayama K, Amano T (1973) Determination of the non-isothermal crystallization rate constant of grafted maleic anhydride and grafted acrylic acid polypropylenes. *J Appl Polym Sci* 17:1031–1041
- Ozawa T (1971) Kinetics of non-isothermal crystallization. *Polymer* 12:150–158
- Ziabicki A (1974) Theoretical analysis of oriented and non-isothermal crystallization. *Colloid Polym Sci* 252:433–447
- Caze C, Devaux E, Crespy A, Cavrot JP (1997) A new method to determine the avrami exponent by dsc studies of non-isothermal crystallization from the molten state. *Polymer* 38:497–502
- Wang D, Gao JG (2006) Melting, nonisothermal crystallization behavior and morphology of polypropylene/random ethylene-propylene copolymer blends. *J Appl Polym Sci* 99:670–678
- Herrero CR, Acosta JL (1994) Effect of poly(epichlorhydrin) on the crystallization and compatibility behavior of poly(ethylene oxide)/polyphosphazene blends. *Polym J* 26:786–796
- De Juana R, Jauregui A, Calahorra E, Cortázar M (1996) Non-isothermal crystallization of poly(hydroxy ether of bisphenol-A)/poly(ϵ -caprolactone), PH/PCL blends. *Polymer* 37:3339–3345
- Lee SW, Ree M, Park CE, Jung YK, Park CS, Jin YS, Bae DC (1999) Synthesis and non-isothermal crystallization behaviors of poly(ethylene isophthalate-co-terephthalate)s. *Polymer* 40:7137–7146
- Wang YJ, Run MT (2009) Non-isothermal crystallization kinetic and compatibility of PTT/PP blends by using maleic anhydride grafted polypropylene as compatibilizer. *J Polym Res* 16:725–737
- Durmus A, Yalçımyuva T (2009) Effects of additives on non-isothermal crystallization kinetics and morphology of isotactic polypropylene. *J Polym Res* 16:489–498
- Chen Y, Zou HW, Liang M (2014) Non-isothermal crystallization study of in-situ exfoliated graphite filled nylon 6 composites. *J Polym Res* 21:417
- Rao IJ, Rajagopal KR (2004) On the modeling of quiescent crystallization of polymer melts. *Polym Eng Sci* 44:123–130
- Tian JH, Yu W, Zhou CX (2006) The preparation and rheology characterization of long chain branching polypropylene. *Polymer* 47:7962–7969
- Liao RG, Yu W, Zhou CX, Yu FY, Tian JH (2008) The formation of gamma-crystal in long-chain branched polypropylene under supercritical carbon dioxide. *J Polym Sci Polym Phys* 46:441–451

38. Martuscelli E, Silvestre C, Abate G (1982) Morphology, crystallization, and melting behavior of films of isotactic polypropylene blended with ethylene-propylene copolymers and polyisobutylene. *Polymer* 23:229–237
39. Karger-Kocsis J, Kallo A, Szafner A, Bodor G, Senyei Z (1979) Morphological study on the effect of elastomeric impact modifiers in polypropylene systems. *Polymer* 20:37–43
40. Kim YC, Kim CY, Kim SC (1991) Crystallization characteristics of isotactic polypropylene with and without nucleating agents. *Polym Eng Sci* 31:1009–1014
41. Choe CR, Lee KH (1989) Nonisothermal crystallization kinetics of poly(etheretherketone) (PEEK). *Polym Eng Sci* 29:801–805
42. Jeziorny A (1978) Parameters characterizing the kinetics of the non-isothermal crystallization of poly(ethylene terephthalate) determined by d.s.c. *Polymer* 19:1142–1144